High altitude (~4520 m amsl) measurements of black carbon aerosols over western trans-Himalayas: Seasonal heterogeneity and source apportionment

S. Suresh Babu,[1] Jai Prakash Chaubey,[1] K. Krishna Moorthy,[1] Mukunda M. Gogoi,[1] Sobhan Kumar Kompalli,[1] V. Sreekanth,[1] S. P. Bagare,[2] Bhuvan C. Bhatt,[2] Vinod K. Gaur,[2] Tushar P. Prabhu,[2] and N. S. Singh[2]

Received 15 August 2011; revised 13 October 2011; accepted 14 October 2011; published 22 December 2011.

[1] The first ever, year-round measurements of aerosol black carbon (BC) over the western part of trans- Himalayas are reported from Hanle (~4520 m above mean sea level). The daily mean BC concentrations varied from as low as 7 ng m^{-3} to as high as 296 ng m^{-3} with an annual average of 77 ± 64 ng m^{-3}, indicating significant BC burden even at free-tropospheric altitudes. Variation with in the day as well as from day to day were highly subdued during winter season (December to February) while they used to be the highest in Spring (March to May). In general, the less frequently occurring high BC values contributed more to the annual and seasonal means, while 64% of the values were below the annual mean. Seasonally, highest BC concentration (109 ± 78 ng m^{-3}) occurred during Spring and lowest (66 ± 42/66 ± 62 ng m^3) during Summer/Winter season(June to August/December to February). Diurnal variations in general were very weak, except during Spring and Summer when the effects of convective boundary layer dynamics is discernible. Back trajectory clustering and concentration weighted trajectory (CWT) analyses indicated that, most time of the year the sampling location is influenced by the advection from West and Southwest Asia, while the contribution from the Indo-Gangetic Plains (IGP) remained very low during Spring and Summer. The seasonal and annual mean BC at Hanle are significantly lower than the corresponding values reported for other Himalayan stations, while they were quite higher than those reported from the South Pole and pristine Antarctic environments.

Citation: Babu, S. S., et al. (2011), High altitude (~4520 m amsl) measurements of black carbon aerosols over western trans-Himalayas: Seasonal heterogeneity and source apportionment, *J. Geophys. Res.*, *116*, D24201, doi:10.1029/2011JD016722.

1. Introduction

[2] In the recent years, investigations of black carbon (BC) aerosols have been receiving special attention primarily due to their property to absorb solar radiations in the atmosphere over a wide spectrum [*Bond and Bergstrom*, 2006; *Jacobson*, 2001], thereby contributing toward global warming [*Ramanathan and Carmichael*, 2008; *Jacobson*, 2001] unlike majority of the other aerosol species which scatter back the radiation [*Penner et al.*, 1998; *Intergovernmental Panel on Climate Change* (*IPCC*), 2007] leading to a cooling effect in the atmosphere. The numerous field experiments (for example INDOEX (Indian Ocean Experiment), ACE-Asia (Aerosol Characterization Experiment–Asia), TRACE-P (Transport and Chemical Evolution over Pacific), ARMEX (Arabian Sea Monsoon Experiment), ICARB (Integrated Campaign for Aerosol gases and Radiation Budget) and W-ICARB (Winter-ICARB)) and long-term ground-based network studies have revealed the role of these absorbing aerosols in imparting global and regional climate forcing. Simulation studies have shown that the regional radiative forcing by aerosols containing significant amount of BC would have strong impacts on the hydrological cycle [*Ramanathan et al.*, 2001] and Indian/Asian summer monsoon [*Lau et al.*, 2006]. Furthermore, BC aerosols are potential environmental and health hazards. Both BC and organic carbon (OC) are carcinogenic and are a major cause of deaths associated with particulate air pollution [*Menon et al.*, 2002]. BC aerosols, lofted above by strong convective motions over tropical landmass, reach well above the atmospheric boundary layer and in the entrainment zone [*Babu et al.*, 2008], where the 'meso stable' conditions are conducive for increased layer lifetime of these aerosols, which in turn results in elevated warming in the atmosphere [*Satheesh et al.*, 2008; *Babu et al.*, 2011]. The effects get amplified when the BC layers occur above the highly reflective clouds [*Seinfeld*, 2008]. Several recent studies have shown that aerosols over the South and Southeast Asia, frequently get lifted well above the boundary layer and low-level clouds [*Welton et al.*, 2002;

[1]Space Physics Laboratory, Vikram Sarabhai Space Centre, Trivandrum, India.
[2]Indian Institute of Astro Physics, Bangalore, India.

0148-0227/11/2011JD016722

Hsu et al., 2003; *Satheesh et al.*, 2008; *Babu et al.*, 2011]. As such, information of BC aerosol characteristics in the free troposphere is very important.

[3] BC aerosols, due to their relatively longer lifetime, are amenable for long-range transport even to remote locations such as the Arctic [*Stohl et al.*, 2006], Antarctica [*Tomasi et al.*, 2007; *Chaubey et al.*, 2010] and even over Himalayan region [*Marinoni et al.*, 2010; *Hyvärinen et al.*, 2009; *Dumka et al.*, 2010]. Deposition of BC over snow and ice over the Polar and Himalayan regions would modify the albedo of snow [*Warren and Wiscombe*, 1980; *Jacobson*, 2004; *Flanner et al.*, 2009; *Clarke and Noone*, 1985]. The Himalayan and Tibetan Plateau Glaciers, which are the largest glaciers out side of the Polar Regions, have shown signs of retreat [*Kulkarni et al.*, 2007]. These glaciers being an important source of fresh water for the millions of population, in the South Asian region, this retreat will have far-reaching consequences. *Mikhailov et al.* [2006] have reported that coatings of snow on BC particles can enhance their absorption of solar radiation by a factor of 2. In the backdrop of the above importance of BC aerosols in the atmospheric thermodynamics, it becomes imperative to investigate aerosol characteristics at high altitudes, especially over the Himalayas. As the South Asian region is believed to be one of the hot spots of BC aerosols [*Lawrence and Lelieveld*, 2010; *Bond et al.*, 2007; *Koch and Hansen*, 2005] and the Himalayas form a natural orographic barrier for its northward dispersion, several field experiments have been recently formulated to measure BC in the Himalayan region [*Lau et al.*, 2006; *Hyvärinen et al.*, 2009; *Marinoni et al.*, 2010; *Dumka et al.*, 2010]. Aerosol measurements from elevated locations have also been carried out from different parts of the globe (besides Himalayas), which include Alps (Jungfraujoch, 3450 m amsl) [*Nyeki et al.*, 1998], Italy (Monte Cimmone, 2165 m amsl) [*Marenco et al.*, 2006], and Arizona (Mt. Lemmon, 2790 m amsl) [*Shaw*, 2007]. Recently, under the framework of Stations at High Altitude for Research on the Environment (SHARE) project [*Lau et al.*, 2008; *Bonasoni et al.*, 2010], several high altitude stations were established, which include National Climate Observatory Pyramid (NCOP; 5079 m amsl), Khumbu Valley (∼4528 m amsl), Namche Bazaar (∼3560 m amsl) in Nepal, in eastern Himalayas, a few stations in Italy (including Monte Cimmone) and Gilgit Baltistan (∼3926 m amsl) in Pakistan. Out of these, only NCOP-Nepal has long-term measurements of aerosols parameters whereas for most of the other stations under SHARE projects, results are yet to emerge. Besides these, long-term measurements of BC are being made over the Himalayas from Nainital (29.4°N; 79.5°E, 1958 m) [*Dumka et al.*, 2010] under the Aerosol Radiative Forcing over India (ARFI) project of ISRO – GBP (Indian Space Research Organization - Geosphere Biosphere Program). Recently, *Hyvärinen et al.* [2009] have reported a two year record of BC aerosols from Mukteshwar (29.43°N, 79.62°E, 2180 m), northeast of Nainital. However, these stations (Nainital and Mukteshwar) have proximity to a fair amount of anthropogenic activities arising out of the adjoining densely populated plains. Airborne measurements of aerosols over Indian mainland under Integrated Campaign for Aerosol Radiation Budget (ICARB) [*Moorthy et al.*, 2008] have demonstrated persistent layer of aerosols in the altitude regions of 2 to 4 km within which BC concentration as well as extinction were comparable or higher than the corresponding values seen at the surface [*Babu et al.*, 2008; *Satheesh et al.*, 2008] and the atmospheric warming due to these aerosol layers exhibited a northward gradient [*Satheesh et al.*, 2008]. With a view to examining this aspect and its climate implication in the light of elevated heat pump hypothesis [*Lau et al.*, 2006], a field experiment, Regional Aerosol Warming EXperiment (RAWEX) was formulated under ISRO-GBP. In a most recent and very important development (under RAWEX), *Babu et al.* [2011], using high altitude balloon measurements, have provided first experimental evidences of the change in the environmental lapse rate due to heating by BC aerosols at an altitude region of 4 to 5 km over central India. In the light of all the above and with a view to characterizing BC aerosols in the free troposphere over remote location, a high altitude aerosol observatory was established in western Indian Himalayas, on Mt. Saraswati at Hanle (32.78°N, 78.96°E and 4520 m amsl; Figure 1 (left)), where the Indian Institute of Astrophysics (IIA) has been operating the Himalayan Chandra Telescope. This observatory also forms an integral part of the ARFI NETwork (ARFINET) stations under ISRO-GBP. Continuous measurements of BC mass concentration are being made from this station. The data for period of 1 year from August 2009 to July 2010 are examined and the results are presented in the paper.

2. Experimental Site

[4] Hanle valley (32.78°N, 78.96°E, ∼4250 m amsl) is located in Leh-Ladakh region of India in the western Indian Himalayas (Figure 1) along the southern slope of the Tibetan Plateau. The sampling location is located atop Mt. Saraswati, at an altitude of 4520 m above mean sea level (amsl) and approximately ∼300 m above the base camp in the Hanle valley. In Figure 1 (right) we show the location of observatory, base camp and other settlements at Hanle. The area around the observatory is mostly rocky, sandy and desert like. There is very little vegetation (like shrubs) which disappears by the end of summer and re-appears only by next spring. Mt. Saraswati is surrounded immediately by valley, which is bound by high mountain peaks, some of which are higher in elevation than the observatory site itself. Mountain peaks surrounding Mt Saraswati experience snow fall, especially during winter (December to February) and summer (June to August), while the snow cover persists over many mountain peaks throughout the year. The valley surrounding Mt. Sraraswati has fields, river and scattered settlements. It is home to a population of ∼1700, with about 20 people living in base camp area, 500 (including children and staff) in S.O.S. (Saviors of Soul) Tibetan School and the rest corresponds to the villagers scattered in valley, in ∼20 colonies distributed over an area of ∼20 km^2 and this constitutes the major, if not the only, source of anthropogenic influence over this vast region. Farming of animals (like Yak, Sheep, Goat and Cow) along with small scale vegetable planting, are the main occupations of the villagers. The Hanle river, fed by melting glaciers during spring and summer, flows through the far end of the valley and becomes dry (frozen) in winter. The experimental location is completely isolated from populated

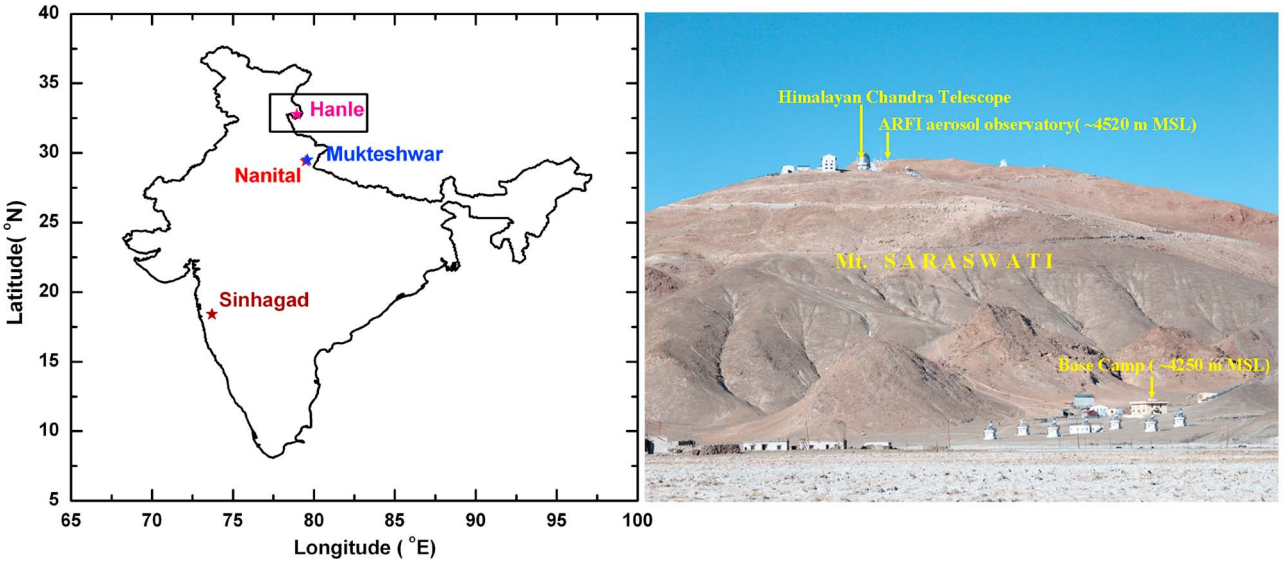

Figure 1. (left) Location map showing Hanle observatory (in rectangle), other high altitude stations in India (Nainital, Mukteshwar and Sinhagadh). (right) Mt Saraswati at Hanle and location of aerosol observatory, Himalayan Chandra Telescope, village, base camp and other facilities at Hanle.

and industrialized cities. The nearest township, Leh (34.25°N, 78°E, 3480 m amsl) having a population of ~27000 is located almost 270 km Northwest of the base camp. Except for short durations (2–3 h in each day, depending on the power requirements), power required for the observatory and the base camp comes from the batteries charged by the solar energy in order to minimize the perturbations to the local environment and maintaining the clean air conditions. As the site is remotely located with minimal anthropogenic activities, elevated from local activity regions and almost similar altitude of free troposphere over plains, it is reasonable to consider it as representative of background free tropospheric regions.

3. Instrumentation and Data Processing

[5] BC mass concentrations (M_{BC}) were estimated regularly from Hanle, using a two channel (370 nm and 880 nm) rack mount aethalometer (model AE 31) of Magee Scientific supplemented with an external pump to cater the need arising out of the low ambient pressure. The ambient air was aspirated from a height (~6 m above the ground), through an inlet tube, first connected to a heated inlet (kept at temperature of ~60°C) and then to the external pump (capable of maintaining a flow rate of 6 lpm at the ambient pressure levels of ~580 hPa). The heated inlet ensured continuous and smooth operation of the aethalometer even during winter time (even when the temperature goes as low as −20°C) and during days with high relative humidity. BC is estimated from the measurements of the change in transmittance of the 880 nm channel. Aethalometer is a field rugged instrument extensively used across the aerosol research community for continuous measurements of ambient BC mass concentration over a variety of environments [see, e.g., *Hansen et al.*, 1984; *Novakov et al.*, 2003; *Moorthy and Babu*, 2006; *Bhugwant et al.*, 2001; *Schmid et al.*, 2006; *Eleftheriadis et al.*, 2009; *Chaubey et al.*, 2010] and the issues associated with aethalometer measured BC (due to particle loading and multiple scattering effects), especially in presence of significant amount of dust or organic aerosols and the fresh emissions from diesel exhaust are well documented [e.g., *Weingartner et al.*, 2003; *Hitzenberger*, 2006; *Nair et al.*, 2009; *Moorthy et al.*, 2009]. At Hanle, the aethalometer was operated under 50% maximum attenuation settings (to keep the loading at a low level) and it measured aged, low concentration of BC (as there are no strong local sources) and hence the above issues are less important. The instrument was operated at a standard mass flow rate of 6 lpm and at a time base of 5 min, so that BC estimates are available every 5 min, on all the days and round the clock. Mass flow rate was 6 lpm (V) under standard temperature (T ~ 293°K) and pressure (P_0 ~ 1013 hPa). However, the ambient pressures being lower than the standard conditions, the measured BC values were corrected [e.g., *Moorthy et al.*, 2004]. The true BC mass concentration (M_{BC}) is

$$M_{BC} = M^{*}_{BC}\left[\frac{P_0 T}{P T_0}\right]^{-1} \quad (1)$$

where M^{*}_{BC} is the instrument measured raw mass concentration at ambient conditions, P_0 and P are the standard and ambient pressure and T_0 and T are the corresponding temperatures.

[6] As the measurements were carried out in a pristine environment, where the BC concentration is expected to be very low, we performed quality check of the data before proceeding with further analysis. Even though the sampling location was ~300 m elevated from the nearby valley, there still could be a very small/remote chance that the activities at the valley, though highly subdued in nature and occurring

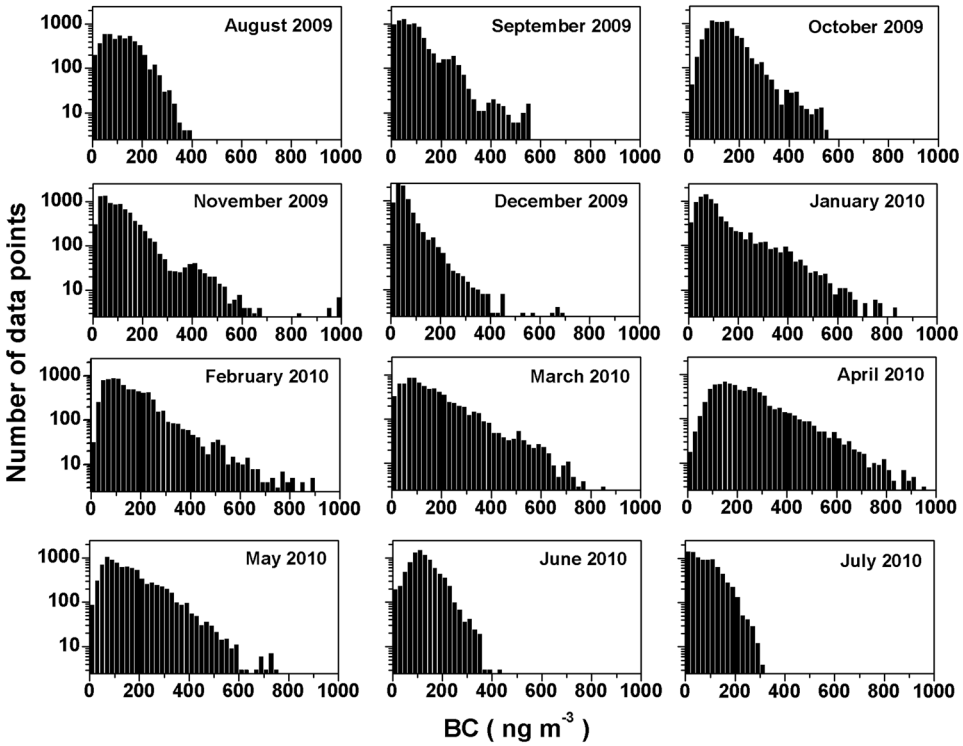

Figure 2. Frequency of occurrence of BC data from Aethalometer for each month starting from August 2009 to July 2010.

downwind the prevailing winds, might have some effect on the measured values, at least under some favorable conditions. This might become important due to the low levels of BC at the station. To check the data for any such artifacts, we have used frequency count method. In Figure 2, we have shown the distribution of the frequency of occurrence of M^{*}_{BC}, separately for each month. The distribution is highly skewed, with most of the values (~81%) lying in the range from 0 to 200 ng m^{-3} over the entire year. Nevertheless, high values (between 200 ng m^{-3} and 400 ng m^{-3}) do occur (~16%), but they are far less numerous and all these values are included in the analysis. However, there were a few values of M^{*}_{BC} going above 400 ng m^{-3} for brief periods and in any month these contributed to <~3% of the total number of samples. These high values, if lasted for more than half an hour duration (6 consecutive points) were considered genuine and were included in the final database, but otherwise excluded as outliers. These data were further examined for any probable impact due to the diesel generators operating in the valley (~300 m down) during the evening and morning hours. The generators are located to the southeast of sampling location, thus downwind for most of the time and operated during fixed timings. Nevertheless, we examined any probable impact of these on the measured BC concentration (again in the view of very low concentration in the ambient). For this we re analyzed the data by removing all the measurements made during the period from the time when the generators were switched on to 30 min after they were switched off, based on the generator logs. It was found that this exercise merely resulted in data gaps; while neither the shape of the diurnal variation nor the daily mean values and standard deviations were affected, there by confirming that the instrument sampled only the background air, uncontaminated by any local effects.

4. Synoptic and Local Meteorology

[7] Being a high altitude mountain station, surrounded by elevated peaks (covered by snow and ice for almost half of the year), and subjected to highly subdued human activities, the prevailing meteorology is important in understanding the aerosol characteristics. The daily meteorological conditions during the study period were inferred from the regular and high resolution measurements of the surface meteorological parameters (temperature (T, °C), pressure (P, hPa), relative humidity (RH, %), wind speed (W_S, m s^{-1}) and wind direction (W_D, degrees measured clockwise from North)), all measured using an automatic weather station at a height of ~3 m above surface and located at the sampling location. Very little precipitation (~10 cm in a year [*Verma et al.*, 2010]), occurs at Hanle and it is mainly accompanied with the snowfall at the site or the nearby mountains. The temporal variations of all these parameters, for the full year, are shown in Figures 3a–3c where the continuous lines show the high resolution data and the solid points correspond to the monthly means estimated from the raw data. The vertical lines passing through the points are the corresponding standard deviations. In Figure 3d we show the seasonal picture of W_S and W_D, in the polar coordinates. As can be seen, the warmest month of the year has been August (mean T ~ 12.4 ± 4.6°C and Tmax ~ 23.1°C) while January was the coldest month (mean T ~ −11.1 ± 3.5°C and Tmin ~ −19.6°C). The ambient pressure showed very little variation; being the highest in September with a value of

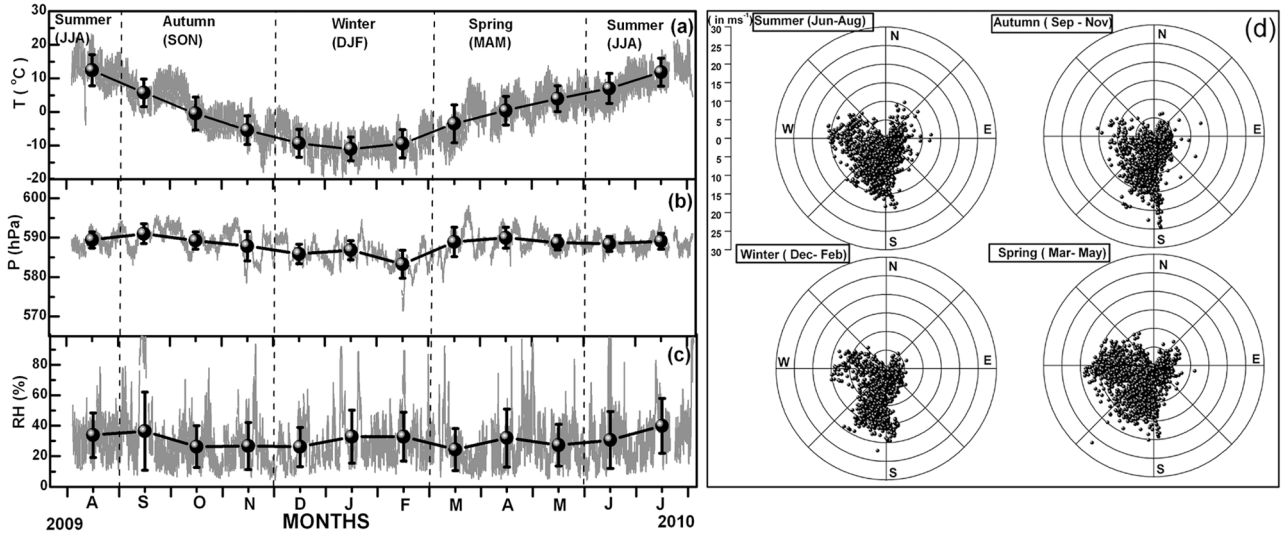

Figure 3. Temporal variation of (a) Temperature (T), (b) Pressure (P) and (c) Relative Humidity (RH) for the full year where the continuous line show the high resolution data and the sphere corresponds to the monthly mean estimated from raw data. The vertical lines are the standard deviation from the mean values. (d) Polar diagrams showing the distribution of hourly mean surface wind for full study period separated in different seasons.

591.0 ± 2.5 hPa and lowest in February (583.3 ± 3.6 hPa). Monthly mean RH varied from a July high (40 ± 18%) to the March low (24 ± 14%). Nevertheless, maximum and minimum values of RH in all the seasons varied in range (4–98%) with most of the time values at the site being <40%, the higher values occurring during highly cloudy periods or during precipitation (rain or snowfall). On the contrary, surface winds varied significantly showing highest during July (mean value of 6.2 ± 4.4 m s^{-1}) and lowest during January (3.8 ± 3.7 m s^{-1}). Predominant wind direction during the measurement period has been from the south and southwest. On a few occasions, winds reached from the West or East direction, but these were far too infrequent and weak. The whole year is divided into four seasons, Summer (June to August, JJA), Autumn (September to November, SON), Winter (December to February, DJF) and Spring (March to May, MAM) and these are also marked in Figure 3. The seasonal variability of meteorological parameters is listed in Table 1.

5. Results and Discussions

5.1. General Features of Temporal Variation

[8] Temporal variations of the daily mean BC mass concentrations (M_{BC}) are shown in Figure 4a, where the vertical lines through the symbols are the standard errors, the dotted line separate different seasons and the continuous line shows the 30-day smoothing for the full year. The short length of the standard error bars indicates the narrow range of fluctuations, generally within a day. The daily mean M_{BC} varied from a minimum of 7 ng m^{-3} to maximum value of 296 ng m^{-3} with an annual mean 77 ng m^{-3}, and standard deviation of 64 ng m^{-3}. It was also found that 64% of the M_{BC} values were below annual mean M_{BC}, indicating a skewed distribution and the low levels of BC existing over western Himalayas. It is also important to note that except for few days in a year (mainly in April and May months), most of the time, daily mean remained < 250 ng m^{-3} at the station. There is a sharp decrease in the daily mean, around the beginning of September, which was due to a heavy rain and snowfall event over the region (including the sampling location), and this is discussed later. Excluding this, BC showed a clear seasonal variation with winter low and spring high. Random variations (day-to-day) were subdued in winter while quite significant during spring compared to summer and autumn. Temporal variation of monthly mean features are shown by the box and whisker plot in Figure 4b, where the solid spheres represent the respective monthly means, the box represent the 25th (lower line), 50th (middle line) and 75th (top line) percentiles, the end of the vertical bars represent the

Table 1. Seasonal Average of Meteorological Parameters, Temperature (T), Relative Humidity (RH), Pressure (P) and Wind Speed (W_S)[a]

Season		T (°C)	P (hPa)	Ws (m s^{-1})	RH (%)
Summer	Mean	10.3 ± 5.1	588.9 ± 2.0	5.5 ± 4.1	34.4 ± 17.5
	Minimum	−3.9	583.9	0	7.01
	Maximum	23.1	594.6	18.79	98.08
Autumn	Mean	−0.2 ± 6.3	589.3 ± 3.2	5.4 ± 4.6	29.6 ± 19.3
	Minimum	−18.1	578.4	0	4.5
	Maximum	16.03	595.7	24.7	98.9
Winter	Mean	−10.0 ± 4.0	585.4 ± 3.2	5.2 ± 4.7	30.5 ± 15.8
	Minimum	−19.6	571.3	0	5.9
	Maximum	0.9	594.7	22.2	91.9
Spring	Mean	0.4 ± 5.5	589.2 ± 2.9	5.9 ± 4.7	27.9 ± 16.1
	Minimum	−15.8	578.6	0	4.5
	Maximum	13.7	598.1	26.7	96.5

[a]Maximum and minimum values recorded in the given season are also listed.

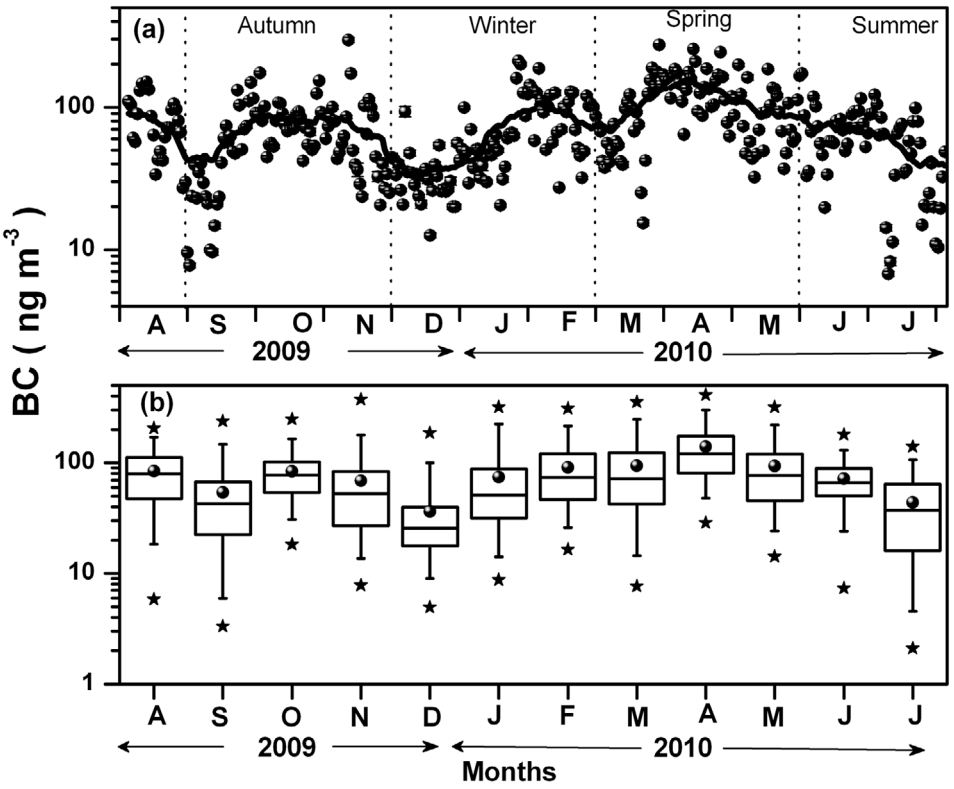

Figure 4. (a) Temporal variation of daily average black carbon (BC) mass concentration for the period August 2009 to July 2010. The spheres present the mean value for the day, and the vertical line passing through them are the standard errors. Different season are separated by dotted line. The solid continuous line shows the 30 day smoothed variation. (b) Box-and-whisker plot of monthly BC concentrations illustrating the mean (sphere), median (the horizontal bar in the box), 25th and 75th percentile (the lower and upper lines of the box), 5 and 95th percentile (end of error bars) and maximum and minimum values for the months (as solid stars).

5th (below the box) and 95th (above the box) percentiles, while stars represents the maximum and minimum values measured for the month. Higher skewed distributions occur with the mean values being higher than the median values (50 percentile) for almost all the months. This means that the high values of M_{BC} play a major role in lifting up the mean, despite the fact that they occur less frequently. The monthly averages ranged from highest value of 140 ± 39 ng m^{-3} in April to the lowest value of 36 ng m^{-3} (with a standard deviation of 39) for December, depicting an annual variation by a factor of 4. The minimum values of M_{BC} remained more or less similar during all the months, while the maximum values showed significant variations; with very high values during spring. BC concentrations that prevail over Hanle have been significantly lower than those reported over far oceanic regions adjoining India by *Babu et al.* [2008, 2010] and those reported from island locations [*Moorthy and Babu*, 2006; *Beegum et al.*, 2008] showing much cleaner environment.

[9] Despite the above, the significant increase is seen (at Hanle) during early spring (March–April). This could be attributed to the increased vertical transport of effluents, confined to the valley during winter by the low level ground based capping inversion, by the increased thermal convection associated with increased solar heating of the mountain surface. The low temperatures, low trade winds inversion, dry and calm ambient winds combined with the low level anticyclone that prevails over the entire Indian plains during winter, inhibits the ventilation and dispersion (vertical) of pollutants from the valley regions, resulting in a build up of BC in lower troposphere as has been reported by several investigators [e.g., *Di Girolamo et al.*, 2004; *Nair et al.*, 2007; *Ramanathan et al.*, 2007] over the adjoining plains and the valleys. With the advent of Spring, the increased thermal convections lead to increased vertical lifting of BC, deeper into the troposphere. Besides, the contribution of upslope thermal winds at high altitude sites vary seasonally (controlled by local meteorological effects), which influences anabatic and katabatic winds during Spring and Summer. The local surface layer over the valley around the observatory might play a role in isolating the sampling site at the peak from the local anthropogenic activities (in the valleys, despite these being very low) especially in winter when temperature remains sub zero and the surface layer inversion remain very low. This has been seen, even visually from the site during winter mornings, when the thin smoke plumes emerging from the scattered houses in the valley remain bound within few meters vertically, and travel horizontally for some distance and then sink to touch the ground, showing the highly confined (in vertical) nature of the local boundary layer. This boundary layer is much shallower than the

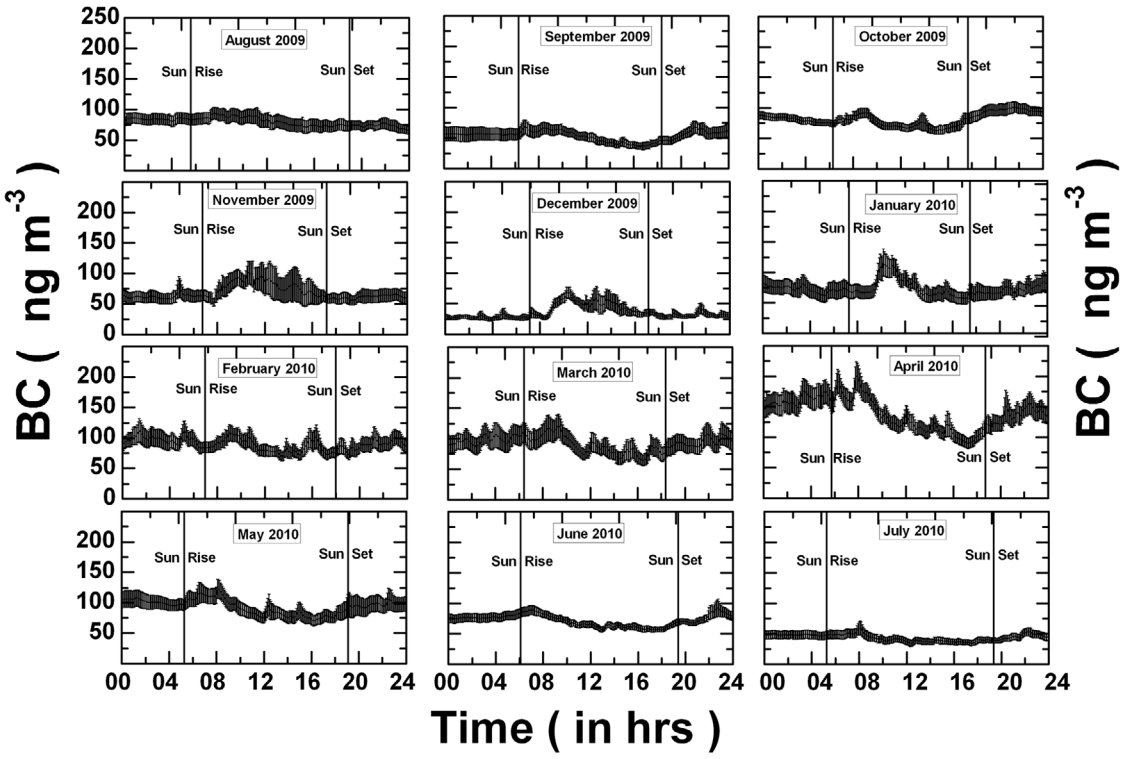

Figure 5. Monthly mean diurnal variations of black carbon (BC) mass concentration obtained for each month from August 2009 to July 2010. The vertical lines in each panel are the time of sun rise and sun set for the respective months.

mountain, there by isolating the measurement site. With the advent of Spring, increasing insolation results in increase in the land/air temperature (Figure 3) and increased convection leading to deepening of the surface layer, which eventually breaks as the season advances, flushing up the particles which have been confined by the shallow capping inversion. The particles, thus lofted, are dispersed spatially by the prevailing winds. This results in a sharp increase in M_{BC} in April, which however decreases further into the summer when the boundary layer deepens further and the particles have already been dispersed and get homogenated with the background. The above, along with the occasional precipitation (snowfall and rain) scavenging of BC, keeps the BC levels to remain lower than the spring time values.

[10] Another important process leading to the variability of BC at Hanle could be the regional meteorology, as Hanle is a part of the very large mountain chain Himalayas. As such, effluents from the somewhat populated, vast sub-Himalayan regions and regions close to western Himalayas might also get transported to the higher altitudes (as discussed above). Part of the BC aerosols thus pumped up, might get transported to the sampling location by favorable regional circulations, favored by the longer life-time of BC aerosol in free troposphere. These processes are more efficient during spring because in summer the regional washouts of the aerosols also became significant. Aerosols confinement near the surface is significant in autumn and winter, due to the low temperatures (Figure 3) and hence the regional contribution also would show seasonal variability. The effect of long range transport, influencing the variability in BC will be examined in later section.

5.2. Diurnal Variations and Their Seasonality

[11] Diurnal variations and their seasonality are also important in understanding the effect of local meteorology and atmospheric boundary layer (ABL) dynamics, as discussed above. The annual picture of monthly averaged diurnal variation of M_{BC} is shown in Figure 5. The vertical lines in each panel mark the local sunrise and sunset times, which show a progressive decrease in the duration of daytime as we move from August to January (as the winter advances) and subsequent increase from February to July as the season changes through spring to summer. The Figure 5 reveals that (1) diurnal variations remain inconspicuous from June through October implying very weak impact of ABL dynamics, (2) a conspicuous pattern with an afternoon high and late night low during November to January showing the role of the dynamical ABL affecting the measurement location during day while the capping surface layer insulating it at night similar to the effects reported by *Dumka et al.* [2010] and (3) a rather strong (in comparison to June–October) diurnal variations with an afternoon low and early morning high during April and May, in line with flushing out of valley bound pollutants by the breaking of capping inversion and subsequent homogenization, discussed above. Despite these the BC levels remain relatively higher during February to May months during all hours of the day. During the period June to October, the nature of the diurnal variations resemble those seen over typical continental locations with an afternoon low and nighttime high, even though the amplitude is very small. This appears to be resulting from the convective boundary layer dynamics, similar to those seen over the

Table 2. Cluster Mean Values of Black Carbon Mass Concentration (M_{BC}, ng m^{-3}) for Different Seasons[a]

Season	Cluster	Originating Location	Percent of Trajectories	Mean M_{BC} (ng m^{-3})
Summer	1	SE	9	18 ± 15
	2	W	82	67 ± 32
	3	NE	9	89 ± 30
Autumn	1	NW	44	76 ± 49
	2	SE	15	32 ± 17
	3	W	41	74 ± 37
Winter	1	SW	28	85 ± 53
	2	W_W	63	63 ± 38
	3	W_N	9	34 ± 13
Spring	1	SW	33	125 ± 58
	2	W_N	17	73 ± 34
	3	W_W	49	110 ± 57

[a]W_N is used for the mean cluster which are shifted northward, while W_W is used for the mean cluster very close to the true west direction of the sampling location.

continents, but at a much subdued strength because of elevation and low thermal gradients (orography). Besides, the sampling location being a hill, the high and variable surface winds (Figure 3) at the location, may result in more efficient 'hand over process' to the free troposphere [*Kossmann et al.*, 1999, 1998] leading to faster dispersion and hence dilution of BC near the surface during summer daytime. More importantly, growth of BC vertical mixing depends on the surface heating, large scale vertical motion, horizontal advection and entrainment at the top of the boundary layer [*Stull*, 1988; *Kalthoff et al.*, 1998]. While the convection starts building up in the morning hours, the orography has its effect on the diurnal variation in the afternoon hours, and the convective boundary layer is independent of topography [*Fiedler et al.*, 2000]. During the evening and throughout the night, surface temperature decreases faster due to the radiative cooling of the ground, resulting in the weakening and collapse of this local boundary layer. Though these would qualitatively explain the weak diurnal variations, more detailed investigations incorporating boundary layer profiling are needed to quantify the arguments. Similar, weak diurnal variations during the period from July to September have also been reported from another high altitude Himalayan station, National Climate Observatory-Pyramid (NCOP)-Nepal [*Marinoni et al.*, 2010]. However, from November to January the diurnal variations appear to be more influenced by the meso-scale ABL with features similar to those experienced at high altitude locations where the BC shows an afternoon peak [*Pant et al.*, 2006; *Venzac et al.*, 2009; *Marinoni et al.*, 2010; *Dumka et al.*, 2010]. It is also noteworthy that, diurnal variations are more pronounced during these months, even though the duration of the day starts decreasing progressively. It is also seen in Figure 2 that the frequency distributions are more skewed toward lower BC values during these months showing the prevalence of cleaner near background conditions at the peak during most of the day. This arises from the shielding by the very shallow winter-surface layer, as discussed earlier, by which the mountain peak is isolated. In addition, the higher air temperature at the sampling location (than the air temperature over surrounding peaks which are taller (>5 km amsl) and snow covered), favors advection of still cleaner air from those regions to the sampling location. This effect also will be more pronounced during Winter, when the day length decreases. While the regional advection reduces during the spring with the reduction in the temperature gradients, it results in the increased thermal convection and allows the aerosol confined in the valley to move to higher heights leading to the pronounced diurnal variations in Spring (April and May). Despite of all the above, the change in the amplitude of the diurnal variation (difference between maximum and minimum M_{BC}) for different months, remained always within limit of 50 ng m^{-3} which means that the modulations by the ABL dynamics are rather weak.

6. Long Range Transport and Source Apportionment

6.1. Effect of Long Range Transport

[12] Remote locations, such as Hanle are ideally suited to examine the impact of long-range transport. The variability in the daily mean BC mass concentration can be either due to the short-term changes (day to day) in the thermal wind (section 5.2) or due to the long range transport or local transport from other regions of Himalayas or a combination of all. Several earlier investigations [*Hindman and Upadhyay*, 2002; *Hegde et al.*, 2007; *Bonasoni et al.*, 2010] have reported that, Himalayan regions are affected significantly by aerosol uplifted by convection, mountain circulation and advected subsequently by the synoptic winds and these effects peak during the spring season. To examine the role of long range transport, 7-day HYSPLIT back trajectories [http://www.arl.noaa.gov/ready.html], ending at 100 m above ground level of the sampling peak (which is ~300 m above the Hanle valley), at 1130 h local time, have been computed. The 7 day period was chosen because of the longer life time of BC expected at these altitudes. Despite the large range of possible trajectory error, the commonly accepted error values are around 20% of the total travel distance [*Moy et al.*, 1994; *Vaughan et al.*, 2002]. The trajectories for different seasons (~90 trajectories in one season) were grouped into three mean clusters following angle-distance algorithm [*Sirois and Bottenheim*, 1995]. The trajectory cluster statistics are listed in Table 2, separated into different seasons, for the whole study period, along with the cluster mean BC values. Noteworthy is that, during the Winter and Spring seasons two mean clusters are almost from the similar direction (i.e., West). To distinguish these clusters we have used W_W for the mean cluster very close to the true west direction of the sampling location and W_N is used for the mean cluster which are shifted northward, from the true West. Our analyses show that major contribution to BC comes from the air mass arriving Hanle from west and southwest of Hanle, i.e., West Asia, Southwest Asia and North African region except perhaps in Spring, when W_N also is significant. There are a few occasions, that too in Summer (9%) and Autumn (15%), when trajectories arrived from the Southeast of location i.e., Indo Gangetic Plain (IGP). Most importantly, BC values at Hanle remained low during these periods indicating that the contribution to BC over Hanle by advection from the IGP is rather insignificant. During Summer, highest BC was associated with trajectories arriving from northeast of the location. During Spring season, trajectories arrived at the location mostly from West Asia and North Africa leading to significant increase in BC at Hanle. Based on the back trajectory

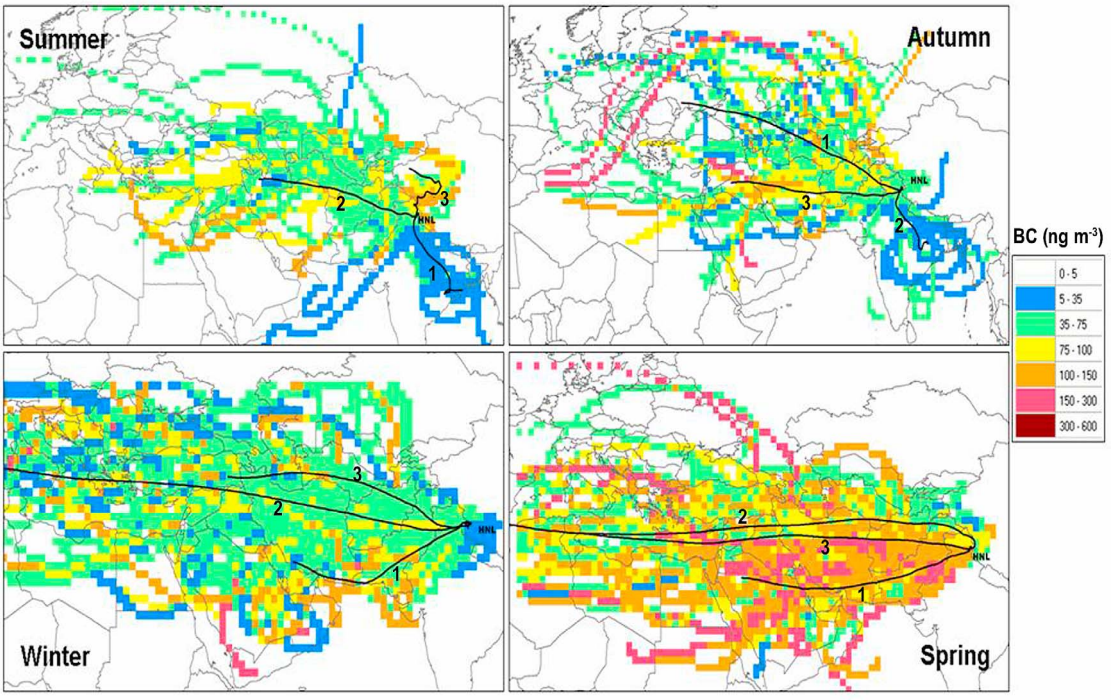

Figure 6. Concentration weighted trajectory (CWT) map for black carbon (BC) mass concentration (ng m^{-3}) during different seasons, along with the mean trajectory clusters (thick lines). Color scale represents the BC mass concentration.

analysis, *Dumka et al.* [2010] have shown that central Himalayas are also influenced by long range transport from Africa and Europe apart from regional pollution, while *Bonasoni et al.* [2010], have reported the influence of long-range transport from the air masses coming from South Asia and IGP at the high altitude station NCOP, located in Eastern Himalayan region.

6.2. Source Apportionment

[13] Even though the cluster analysis gives quantitative differences between the different clusters in terms of aerosol parameters, it is not effective in better delineation of potential source regions. *Seibert et al.* [1994] developed the concentration weighted trajectory (CWT) method, which assigns the concentration values at the receptor site to the respective backward trajectories. To calculate CWT, the whole geographic region covered by the trajectories is divided into an array of grid cells (defined by the cell indices i and j) whose size is dependent on the geographical scale encountered. Each grid cell is assigned a residence time weighted concentration from the measured sample associated with the trajectories that crossed that grid cell as follows

$$C_{ij} = \frac{1}{\sum_{l=1}^{M} \tau_{ijl}} \sum_{l=1}^{M} C_l \tau_{ijl} \qquad (2)$$

where, C_{ij} is the average weighted concentration in the ijth cell, l is the index of the trajectory, M is the total number of trajectories, C_l is the concentration observed on arrival of trajectory l and τ_{ijl} is the time spent in the ijth cell by trajectory l. The time a trajectory spends in a cell could be represented by the number of trajectory segments located in that cell. A high value of C_{ij} implies that air parcels traveling over the ijth cell would be, on an average, associated with high concentration at the receptor (more details are available from *Gogoi et al.* [2011]) with an overall implicit consideration that the receptor site is not a source. Following this, the CWTs were calculated for BC mass concentrations and are superposed in Figure 6 for their seasonal features along with mean trajectories. The analyses confirm quantitatively that the most important potential source region influencing Hanle is the west Asia, Arabian desert regions and north African regions, especially during Spring season (when BC concentration is the highest of year), while the advection of aerosols from the IGP region has least influence at Hanle in any season. Weak to moderate source contributions also occur from locations West to the Hanle (which is maximum during the spring season) resulting into the high values of BC mass concentration at the sampling site. Overall the receptor site is influenced by advection from the west (as discussed above) but the amount of contribution varies from season to season, the contribution being highest in Spring, decreases in summer, followed by a slight increase during the autumn season and becomes almost insignificant during the winter season.

7. Comparison of Hanle BC With Values at Other Locations

[14] Even though the BC concentration is expected to be very low over Hanle due to its elevation, and remoteness,

Table 3. Black Carbon Mass Concentrations (in ng m^{-3}) at Different Locations

Station Name	Latitude and Longitude	Altitude (m)	Summer		Autumn		Winter		Spring		References
			Mean	Stdev	Mean	Stdev	Mean	Stdev	Mean	Stdev	
Himalayan/Tibetan Region (Third Pole)											
NCOP Nepal	27.95N 86.82E	5079	56	75	137	126	125	147	320	469	*Marinoni et al.* [2010]
Nam Co	30.77N 90.99E	4730	M-O[a]	M-O[a]	M-O[a]	M-O[a]	N-J[b]	N-J[b]	N-J[b]	N-J[b]	*Ming et al.* [2010]
Hanle	32.78N 78.95E	4520	63	20	72	33	68	42	110	57	Present study
Mukteshwar	29.43N 79.61E	2180	532	369	692	488	786	706	1216	796	*Hyvärinen et al.* [2009]
Nainital	29.40N 79.5E	1958	530	20[c]	1030	40[c]	1100	60[c]	1340	50[c]	*Dumka et al.* [2010]
Dehradun	30.34N 78.04E	700	2675	908	3041	1643	6737	2237	4233	1738	ARFINET unpublished data
Antarctica and Arctic											
South Pole[d]	90S	2840	1.18	-	0.21	-	0.4	-	0.98	-	*Bodhaine* [1995]
Maitri	70.77S 11.73E	123	-	-	-	-	75	33	-	-	*Chaubey et al.* [2010]
Larsemann Hills	69.73S 76.19E	48	-	-	-	-	13	5	-	-	*Chaubey et al.* [2010]
McMurdo	77.85S 166.68E	-	-	-	-	-	20–300	-	-	-	*Hansen et al.* [2001]
Swoya	69S 33E	-	6	2	4.4	0.4	9	1	8	2	*Hara et al.* [2008]
Zeppelin	78.9N 11.88E	474	9.3	-	13	-	50	-	56	-	*Eleftheriadis et al.* [2009]
Alert	82.5N 62.5W	210	8	-	-	-	96	-	-	-	*Sharma et al.* [2004]
Other High Altitude/Background Regions											
Sinhagad Pune, India	18.35N 73.75E	1450	1200	-	-	-	3200	-	-	-	*Safai et al.* [2007]
Jungfraujoch[d] Alps, Switzerland	46.55N 7.98E	3454	6.3	3.5	13.7	7.64	43.3	16.9	8.3	2.0	*Nyeki et al.* [1998]
Mauna Loa[d] Hawaii, U.S.	19.54N 155.58W	3400	4.02	2.56	1.87	0.77	3.36	3.97	15.44	9.50	*Bodhaine* [1995]
La Reunion East of Madagascar	21.5S 55E	151	41	18	23	13	23	13	41	18	*Bhugwant et al.* [2001]
ARFINET Stations Over Indian Mainland											
Bangalore	12.97N 77.59E	960	1885	1650	3485	1855	3430	2330	4025	1515	*Satheesh et al.* [2011]
Hyderabad	17.48N 78.40E	557	2584	322	3605	604	6805	544	4787	1244	ARFINET unpublished data
Pune	18.54N 73.85E	457	1310	-	6040	-	7380	-	3250	-	*Safai et al.* [2007]
Delhi	28.58N 77.2E	260	24870	3270	22000	5520	12400	6340	12470	1270	*Rai et al.* [2002]
Dibrugarh	27.3N 94.6E	111	3400	900	10900	3900	16300	1400	7500	1500	*Pathak et al.* [2010]
Ahembdabad	23.5N 72.60E	55	1500	800	7300	3700	5500	2800	2200	1000	*Ganguly and Jayaraman* [2006]
Kanpur	26.40N 80.30E	50	-	-	-	-	9800	2750	4250	1770	*Nair et al.* [2007]
Kharagpur	22.50N 87.50E	28	-	-	-	-	13460	3930	3500	1410	*Nair et al.* [2007]
Trivandrum	8.55N 76.94E	10	2010	66[c]	3460	19[c]	5680	210[c]	2620	14[c]	*Krishna Moorthy et al.* [2007]

[a]Concentration for May to October: 100 ± 78 ng m^{-3}.
[b]Concentration for November to January: 60 ± 53 ng m^{-3}.
[c]These values are standard errors.
[d]These values are calculated from absorption coefficients.

it would be interesting and important to compare it with the values reported elsewhere over Himalayas, other remote and high altitudes locations, as well as over Indian plains. It is also important from the stand point of BC getting deposited (by wash out and/or deposition) on snow and glaciers. We examined the available seasonal mean values of M_{BC} at all the 'three' poles (Himalayas, Antarctic and Arctic), other high altitude and background locations in the Himalayas and elsewhere, and other ARFINET stations over Indian plains. These are listed in Table 3.

7.1. Himalayan Locations

[15] The most obvious result emerging from Table 3 is that Hanle records the lowest BC concentration among the different Himalayan stations and hence represents a relatively more pristine condition. The annual mean BC concentration at Hanle (77 ± 64 ng m^{-3}) is half of the 2-year averaged value (160.5 ± 296 ng m^{-3}) reported for NCOP-Nepal [*Marinoni et al.*, 2010], despite the NCOP being more elevated than Hanle. Notwithstanding this, the seasonal trends were quite similar. The mean BC over Hanle compares well with the values (80 ± 65 ng m^{-3}) reported from Nam Co station (~4730 m amsl) over Tibetan Plateau [*Ming et al.*, 2010], located further east of Hanle but north of NCOP-Nepal, even though, the values reported by *Ming et al.* [2010] corresponds to comparable altitudes, are limited only for few months and do not give clear seasonal characteristics. The annual/seasonal mean BC at Hanle is almost 1/10th of the 1-year average value (806 ± 590 ng m^{-3}) reported for Mukteshwar [*Hyvärinen et al.*, 2009] and Nanital (825 ± 40 ng m^{-3}) [*Dumka et al.*, 2010]; however these stations are at much lower elevation of ~2 km. Coming further down, the mean values at Dehradun (at the foothills of Himalayas), BC concentrations reaches over 2000 ng m^{-3} in all the seasons (ARFINET unpublished data).

7.2. Polar Regions

[16] The annual mean value of BC at Hanle compares well with that reported for the Indian Antarctic station Maitri (70.77°S, 11.73°E) during the southern hemispheric summer [*Chaubey et al.*, 2010] but is significantly higher than the values reported from the Larsemann hills (a very pristine location in Antarctica). The Hanle values are also significantly higher than the values reported by *Bodhaine* [1995]

(almost 15 years prior to our measurements) for the south pole and Swoya station in Antarctica (ranged between 0 to 176 ng m^{-3} [*Hara et al.*, 2008]), thereby providing probable evidences of the anthropogenic influences over the continents being felt as far as the Himalayas and as high as ~5 km. Contrary to more inhabited and anthropogenically perturbed region of Antarctica (McMurdo) the range of BC values [*Hansen et al.*, 2001] were quite comparable to those seen at Hanle. Similarly, winter BC concentrations at Hanle are comparable to the long-term averaged winter values of Canadian Arctic region, Alert [*Sharma et al.*, 2004], and Norwegian Arctic region, Zeppelin [*Eleftheriadis et al.*, 2009], while the summer values are marginally higher. In short, Hanle BC values are comparable to the mean values over the pristine environments of the Polar regions subjected to subdued human activities

7.3. Other Background Locations

[17] In contrast to above, the seasonal mean values of BC for other Indian continental high altitude station Sinhagad (~1450 m amsl), Pune [*Safai et al.*, 2007] were remarkably higher in all seasons despite it being 1.5 km amsl, owing to probably the strong influence of the adjoining cities. Comparing with the values reported from other high altitude locations elsewhere, such as Jungfraujoch (Swiss Alps, ~3450 m amsl) [*Nyeki et al.*, 1998], La Reunion Island (~151 m amsl) [*Bhugwant et al.*, 2001] and Mauna Loa (~3400 m amsl) [*Bodhaine*, 1995], the Hanle values are found to be higher in all seasons. However, these values are reported based on measurements carried out 10 to 15 years prior to the present investigation.

7.4. Comparison With Other ARFINET Stations (Over India Mainland)

[18] Though no surprises are expected, we compared in Table 3, the Hanle BC values with those reported from the ARFINET stations over different environments over the Indian mainland. BC concentration at the mainland stations, Bangalore (Urban) [*Satheesh et al.*, 2011], Hyderabad (Urban, ARFINET unpublished data), Pune (Urban) [*Safai et al.*, 2007], Delhi (Urban) [*Rai et al.*, 2002], Dibrugarh (Remote) [*Pathak et al.*, 2010], Ahembdabad (Urban) [*Ganguly and Jayaraman*, 2006], Kanpur (Urban) [*Nair et al.*, 2007], Kharagpur (Remote) [*Nair et al.*, 2007] and Trivandrum (Semi Urban) [*Krishna Moorthy et al.*, 2007], remained significantly higher than the values at Hanle, in any season. However, interestingly, excluding the mega city Delhi (where the local emissions are much higher), BC showed a decrease from Autumn/Winter to Spring/Summer almost opposite to the seasonal trend seen at Hanle which is the manifestation of the ABL dynamics. The shallow ABL over Indian mainland during Winter [*Nair et al.*, 2007; *Beegum et al.*, 2009; *Gogoi et al.*, 2009], results in a vertical confinement of species leading to the high concentration of BC over these stations during Autumn/Winter, while during Spring and Summer there occurs a significant vertical dispersion of aerosols from surface to free troposphere due to increased thermal convections, leading to a handover of BC from boundary layer to free troposphere, where they would be dispersed spatially with the synoptic winds. These, might be also contributing for the observed seasonality at Hanle (Spring high).

8. Discussion

[19] High altitude regions (of the Himalayas), far removed from the anthropogenic influences, are considered pristine environments, same time very sensitive and important to the climate change. The prevailing dry climate of these regions, making them the so-called 'mountain deserts' with very limited precipitation, are conducive for very slow removal of aerosols from the atmosphere especially in the accumulation regime. The longer lifetime enhances the aerosol forcing on regional climate [*Chung and Seinfeld*, 2005; *Kanakidou et al.*, 2005; *Sun and Ariya*, 2006]. Given this context, accurate and detailed knowledge of composite aerosol characteristics in general, and BC aerosols, in particular, assumes importance over the Himalayas. Being considered as the second largest contributor to global warming after greenhouse gases [*Jacobson*, 2001; *Ramanathan and Carmichael*, 2008], BC aerosol absorption has a special role over the Himalayan regions, where the average mountain altitude is above ~5 km over a large area. Simulation studies have shown that strong absorption by elevated aerosols is capable of producing significant changes to the Asian Summer monsoon through processes such as elevated heat pump (EHP) [*Lau et al.*, 2006]. The role of long-range transport during Spring in bringing-in BC (and other aerosols) from the west (Asia, Africa, Arab and Europe) over the Himalayas, as evidenced in our study, assumes great significance in this context. Our studies have shown that, these regions of Himalayas are more impacted by advection (of aerosols) from the West and Southwest, rather than from the Indo-Gangetic Plains (IGP), as has been suggested by some studies for Eastern Himalayan regions [*Marinoni et al.*, 2010; *Bonasoni et al.*, 2010]. Not only that, many observation showed existence of aerosol layers having a vertical extent of ~3 km [*Ramanathan and Crutzen*, 2003; *Bonasoni et al.*, 2010], extending from Indian Ocean to Himalayan region, which are capable of influencing the air quality and regional as well as global climate. Recent estimates [*Bond et al.*, 2007] have shown high BC emissions over South Asian Region. It is possible that the increase of BC in spring and summer (when solar radiation is abundant at these altitudes) would enhance the atmosphere warming due to absorption by these BC particles. The advection of warmer air mass from the Southeast Asia over the Himalayan region would add to this warming over these regions [*Meehl et al.*, 2008; *Ramanathan et al.*, 2007]. Several experimental campaigns are being conducted recently to understand the characteristics of BC over the Himalayas under the Joint Aerosol Monsoon Experiment [JAMEX, *Lau et al.*, 2008], such as ARP (Aerosol Research Project), CTCZ (Continental Tropical Convergent Zone), STORM (Severe Thunderstorm Observations and Regional Modeling), MAHASRI (Monsoon Asian Hydro-Atmospheric Science Research and Prediction Initiative), ABC (Atmospheric Brown Cloud), EAST-AIRE (East Asian Study of Tropospheric Aerosol: An International Regional Experiment), SHARE-Asia (Stations of High Altitude for Research on the Environment in Asia) and RAJO-MEGHA (Radiation, Aerosol Joint Observations –

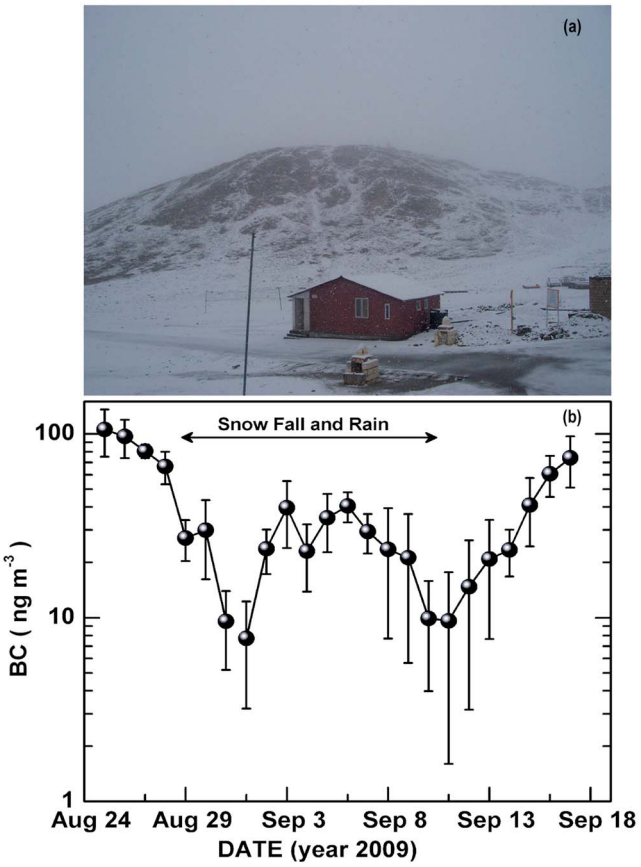

Figure 7. (a) View of nearby areas of Mt. Saraswati from the base camp during the snowfall event. (b) Daily average black carbon (BC) mass concentration from 25th September 2009 to 17th September 2009. The vertical bars are the standard deviation from the mean value and the duration of event is shown with the double sided arrow.

Monsoon Experiments over the Gangetic Himalayas Area) and to analyze the impact on the monsoon system. Recent airborne measurements of vertical profiles of aerosol extinction and BC over the Indian region during Integrated Campaign for Aerosols, gases and Radiation Budget (ICARB) [*Babu et al.*, 2008; *Satheesh et al.*, 2008] have shown elevated layers of BC over several parts of India and also revealed a meridional gradient in the atmosphere warming (due to absorption by these layers) from the Indian ocean to central continent. More recently, high altitude balloon measurements carried out as a part of Regional Aerosol Warming EXperiment (RAWEX) of ISRO-Geosphere Biosphere Program, have shown existence of a strong layer of BC in the altitude region between 4 and 5 km over central India during Spring, which resulted in sharp decrease in the environmental lapse rate in that region [*Babu et al.*, 2011], thereby increasing the stability of atmosphere and lifetime of the BC layer. Viewed in the backdrop of all the above, our observations from Hanle (~4.52 km amsl), reveal two important findings; (i) The annual variation, showing a peak in BC concentration in Spring when the BC concentration is nearly twice as high as the Winter/Autumn values, almost in line with the observation of elevated layers between 4 to 5 km over central Indian region, and (ii) despite of these similarity, the absolute concentrations of BC are significantly lower than what was reported by *Babu et al.* [2008, 2011] over the mainland. These findings, coupled with the values of BC from different Himalayan, sub-Himalayan regions and Indian continent listed in Table 3, brings in several interesting possibilities. While the vertical distribution of BC shows higher values at free tropospheric heights in Spring and Summer over the vast region of India, its absolute magnitude appears to have a sharper latitudinal/longitudinal variations. Furthermore, the observation of a sharp decrease in the surface BC concentration over the plains (ARFINET station in Table 3, except the urban centers which acts as sources) from Winter to Spring and almost an opposite trend of a sharp increase (though of a lesser magnitude, but by a similar factor) over the Himalayan region raises the possibility that at least part of the boundary layer BC is being pumped up to the free troposphere by the convective processes in the atmospheric boundary layer of the tropics.

[20] Our observations from Hanle have another implication to Himalayas (considered as the "third pole") which are the largest source of glaciers, which account for the highest deposition of fresh water outside the polar regions. Continued deposition of BC on this snow and glacier would lower its surface reflectance and promote faster melting of glaciers, resulting into perturbation of radiation budget and hence climate over these region through snow albedo feedback [*Clarke and Noone*, 1985; *Hansen and Nazarenko*, 2004; *Flanner et al.*, 2009]. Recent observations [*Kulkarni et al.*, 2007] have shown an overall reduction in glacial area from 2077 km^2 (in 1962) to 1628 km^2 (in 2007) and an overall deglaciation of 21%. Even though BC may not be entirely responsible for the retreat, abundance of BC concentration at the glacier altitudes and the consequent warming of the atmosphere in these regions would be among the factors contributing to retreat of Himalayan glaciers [*Ramanathan and Carmichael*, 2008; *IPCC*, 2007] This demands for the estimation of BC in the atmosphere as well as in the snow and ice over the Himalayas. In this context, we examined the impact of the short event which occurred during 25th August 2009 to 12th Sep 2009 over Hanle when Mt. Saraswati and near by areas experienced a rare, but extended snowfall. In Figure 7a, we show the view of nearby areas of Mt. Saraswati from the base camp during the snowfall event, while in Figure 7b, the day-to-day variations in daily mean BC during these days are shown, with the vertical bars representing the standard deviations and the points are the daily mean values. A sharp and consistent decrease in the mean BC concentration occurred with the advent of the snowfall and the concentration reduced from 105 ng m^{-3} on 25th August 2009 to very low values (~7 ng m^{-3} by 1st September 2009) comparable to the values at the South Pole. Subsequently there was a small build up, from 2nd September 2009 (~23 ng m^{-3}) to 6th September 2009 (~38 ng m^{-3}) due to breaks in snowfall, nevertheless; BC remained at levels significantly lower than annual mean value (~77 ng m^{-3}). In this type of dry atmosphere, snow fall is better process for scavenging [*Chaubey et al.*, 2010, 2011] of BC than other processes of precipitation scavenging. This may be one reason for the slight increase in M_B after 2nd September 2009. It again started decreasing from 7th September 2009 as the snowfall intensified, and by 12th September 2009 and the BC concentration reached again as low as 9 ng m^{-3}. It took

nearly 7 days, after the event, for BC to reach near the mean values existed prior to the event showing the non-local sources being the chief contributor to the replenishment. This is in contrast to a similar case reported by *Chaubey et al.* [2010] over Antarctic station Maitri, where the replenishment was rapid and mainly attributed to the activities at stations in and around Maitri. The BC scavenged from the atmosphere will become part of snow and will result in change of snow albedo. Based on the ice core data analysis, *Ming et al.* [2008] have shown that the average BC concentration in Himalayan snow was up to 80 ng m^{-3}. We however, could not do an analysis as the snowfall was unexpected. Further observations are needed for better understanding of deposition processes onto Himalayan region and their effects.

9. Summary/Conclusion

[21] The present work represents the first results of temporal (diurnal and seasonal) variations and source identification of aerosol Black Carbon (BC), using one year data (1 August 2009 to 31 July 2010) from the ARFINET observatory, at Hanle, the only high altitude station in western Indian Himalayas. Our important findings are as follows.

[22] 1. Daily mean BC concentration varied from a low value of 7 ng m^{-3} to a high value of 296 ng m^{-3} with an annual mean of 77 ng m^{-3}, and standard deviation of 64 ng m^{-3}. About ~64% of the values were below annual mean BC, indicating that the high annual mean arises from the less frequently occurring high BC concentrations. Seasonally, the highest concentration is in Spring (109 ± 78 ng m^{-3}) and the lowest in winter (~36 ng m^{-3} (with a standard deviation of 39)).

[23] 2. Diurnal variation in BC mass concentration remained inconspicuous from June through October, while it showed afternoon high and late night low during November to January, indicating the presence of a shallow surface layer over the valley. Strong diurnal variation associated with a convective atmospheric boundary layer is observed during April and May.

[24] 3. Major contribution toward the BC mass concentration at Hanle is associated with the air mass arriving from West and South West of the sampling location. BC concentration remained low when the trajectories arrived from South East of location including the Indo Gangetic Plains. Concentrated Weighted Trajectory analysis showed that the potential sources influencing western Himalayas are located West of the sampling location and the source strength varies from maximum during Spring and minimum during Winter.

[25] 4. Despite similarity in the seasonal trends, Hanle records the lowest BC concentration than other Himalayan location. BC levels at Hanle are comparable to other pristine environment (like Antarctica and Arctic) on Earth with subdued human activities.

[26] 5. Higher concentration of BC in Spring and its subsequent deposition on snow and ice cover with efficient long range transport and availability of solar energy during this season may have strong climate consequences, resulting into the warming of atmosphere enhancing the retreat of glaciers.

[27] **Acknowledgments.** This study is a part of the RAWEX under Aerosol Radiative Forcing over India (ARFI) project of ISRO-GBP. We thank Director of Indian Institute of Astrophysics, Bangalore, for rendering their support for the observations. Thanks are also due to entire staff of Indian Astronomical Observatory - Hanle for invaluable help during the installation of instruments and observations. The technical support provided by P.P. Pramod with the instruments at Hanle is acknowledged gratefully. The authors greatly acknowledge the NOAA Air Resources Laboratory (ARL) for the provision of the HYSPLIT transport and dispersion model and/or READY Web site (available online at http://www.arl.noaa/gov/ready.htm) used in this publication.

References

Babu, S. S., S. K. Satheesh, K. K. Moorthy, C. B. S. Dutt, V. S. Nair, D. P. Alappattu, and P. K. Kunhikrishnan (2008), Aircraft measurements of aerosol black carbon from a coastal location in the north-east part of peninsular India during ICARB, *J. Earth Syst. Sci.*, *117*, 263–271, doi:10.1007/s12040-008-0030-1.

Babu, S. S., K. K. Moorthy, and S. K. Satheesh (2010), Vertical and horizontal gradients in aerosol black carbon and its mass fraction to composite aerosols over the east coast of peninsular India from aircraft measurements, *Adv. Meteorol.*, *2010*, 812075, doi:10.1155/2010/812075.

Babu, S. S., K. K. Moorthy, R. K. Manchanda, P. R. Sinha, S. K. Satheesh, D. P. Vajja, S. Srinivasan, and V. H. A. Kumar (2011), Free tropospheric black carbon aerosol measurements using high altitude balloon: Do BC layers build their own homes up in the atmosphere?, *Geophys. Res. Lett.*, *38*, L08803, doi:10.1029/2011GL046654.

Beegum, S. N., K. K. Moorthy, S. S. Babu, G. M. Kumar, S. Sampath, and V. R. Aneesh (2008), Impact of mountain grass land fire on the concentration of aerosol black carbon and carbon monoxide near the surface at a coastal remote location, *Atmos. Res.*, *88*, 45–55.

Beegum, S. N., K. K. Moorthy, and S. S. Babu (2009), Aerosol microphysics over a tropical coastal station inferred from the spectral dependence of Angstrom wavelength exponent and inversion of spectral aerosol optical depths, *J. Atmos. Sol. Terr. Phys.*, *71*, 1846–1857, doi:10.1016/j.jastp.2009.07.004.

Bhugwant, C., M. Bessafi, E. Riviere, and J. Leveau (2001), Diurnal and seasonal variation of carbonaceous aerosols at a remote MBL site of La Reunion island, *Atmos. Res.*, *57*, 105–121, doi:10.1016/S0169-8095(01)00066-7.

Bodhaine, B. A. (1995), Aerosol absorption measurements at Barrow, Mauna Loa and the South Pole, *J. Geophys. Res.*, *100*, 8967–8975, doi:10.1029/95JD00513.

Bonasoni, P., et al. (2010), Atmospheric brown clouds in the Himalayas: First two years of continuous observations at the Nepal Climate Observatory-Pyramid (5079 m), *Atmos. Chem. Phys.*, *10*, 7515–7531, doi:10.5194/acp-10-7515-2010.

Bond, T. C., and R. W. Bergstrom (2006), Light absorption by carbonaceous particles: An investigative review, *Aerosol Sci. Technol.*, *40*, 27–67, doi:10.1080/02786820500421521.

Bond, T. C., E. Bhardwaj, R. Dong, R. Jogani, S. Jung, C. Roden, D. G. Streets, and N. M. Trautmann (2007), Historical emissions of black and organic carbon aerosol from energy-related combustion, 1850–2000, *Global Biogeochem. Cycles*, *21*, GB2018, doi:10.1029/2006GB002840.

Chaubey, J. P., K. K. Moorthy, S. S. Babu, V. S. Nair, and A. Tiwari (2010), Black carbon aerosols over coastal Antarctica and its scavenging by snow during the Southern Hemispheric summer, *J. Geophys. Res.*, *115*, D10210, doi:10.1029/2009JD013381.

Chaubey, J. P., K. K. Moorthy, S. Suresh Babu, and V. S. Nair (2011), The optical and physical properties of atmospheric aerosols over the Indian Antarctic stations during southern hemispheric summer of the International Polar Year 2007–2008, *Ann. Geophys.*, *29*, 109–121, doi:10.5194/angeo-29-109-2011.

Chung, S. H., and J. H. Seinfeld (2005), Climate response of direct radiative forcing of anthropogenic black carbon, *J. Geophys. Res.*, *110*, D11102, doi:10.1029/2004JD005441.

Clarke, A., and K. Noone (1985), Soot in the Arctic: A cause for perturbation in radiative transfer, *Atmos. Environ.*, *19*(12), 2045–2053, doi:10.1016/0004-6981(85)90113-1.

Di Girolamo, L., T. C. Bond, D. Bramer, D. J. Diner, F. Fettinger, R. A. Kahn, J. V. Martonchik, M. V. Ramana, V. Ramanathan, and P. J. Rasch (2004), Analysis of Multi-angle Imaging SpectroRadiometer (MISR) aerosol optical depths over greater India during winter 2001–2004, *Geophys. Res. Lett.*, *31*, L23115, doi:10.1029/2004GL021273.

Dumka, U. C., K. K. Moorthy, R. Kumar, P. Hegde, R. Sagar, P. Pant, N. Singh, and S. S. Babu (2010), Characteristics of aerosol black carbon mass concentration over a high altitude location in the Central Himalayas from multi-year measurements, *Atmos. Res.*, *96*, 510–521, doi:10.1016/j.atmosres.2009.12.010.

Eleftheriadis, K., S. Vratolis, and S. Nyeki (2009), Aerosol black carbon in the European Arctic: Measurements at Zeppelin station, Ny-Alesund,

Svalbard from 1998–2007, *Geophys. Res. Lett.*, *36*, L02809, doi:10.1029/2008GL035741.

Fiedler, F., I. Bischoff-Gauß, N. Kalthoff, and G. Adrian (2000), Modeling of the transport and diffusion of a tracer in the Freiburg-Schauinsland area, *J. Geophys. Res.*, *105*(D1), 1599–1610, doi:10.1029/1999JD900911.

Flanner, M. G., C. S. Zender, P. G. Hess, N. M. Mahowald, T. H. Painter, V. Ramanathan, and P. J. Rasch (2009), Springtime warming and reduced snow cover from carbonaceous particles, *Atmos. Chem. Phys.*, *9*, 2481–2497.

Ganguly, D., and A. Jayaraman (2006), Physical and optical properties of aerosols over an urban location in western India: Implications for shortwave radiative forcing, *J. Geophys. Res.*, *111*, D24207, doi:10.1029/2006JD007393.

Gogoi, M. M., K. K. Moorthy, S. S. Babu, and P. K. Bhuyan (2009), Climatology of columnar aerosol properties and the influence of synoptic conditions: First-time results from the northeastern region of India, *J. Geophys. Res.*, *114*, D08202, doi:10.1029/2008JD010765.

Gogoi, M. M., B. Pathak, K. K. Moorthy, P. K. Bhuyan, S. S. Babu, K. Bhuyan, and G. Kalita (2011), Multi-year investigations of near surface and columnar aerosols over Dibrugarh, northeastern location of India: Heterogeneity in source impacts, *Atmos. Environ.*, *45*, 1714–1724, doi:10.1016/j.atmosenv.2010.12.056.

Hansen, A. D. A., H. Rosen, and T. Novakov (1984), The aethalometer, an instrument for the real-time measurement of optical absorption by aerosol particles, *Sci. Total Environ.*, *36*, 191–196, doi:10.1016/0048-9697(84)90265-1.

Hansen, A. D. A., D. H. Lowenthal, J. C. Chow, and J. G. Watson (2001), Black carbon aerosol at McMurdo station, Antarctica, *J. Air Waste Manage. Assoc.*, *51*, 593–600.

Hansen, J., and L. Nazarenko (2004), Soot climate forcing via snow and ice albedos, *Proc. Natl. Acad. Sci. U. S. A.*, *101*, 423–428, doi:10.1073/pnas.2237157100.

Hara, K., K. Osada, M. Yabuki, M. Hayashi, T. Yamanouchi, M. Shiobara, and M. Wada (2008), Measurement of black carbon at Syowa station, Antarctica: Seasonal variation, transport processes and pathways, *Atmos. Chem. Phys. Discuss.*, *8*, 9883–9929, doi:10.5194/acpd-8-9883-2008.

Hegde, P., P. Pant, M. Naja, U. C. Dumka, and R. Sagar (2007), South Asian dust episode in June 2006: Aerosol observations in the central Himalayas, *Geophys. Res. Lett.*, *34*, L23802, doi:10.1029/2007GL030692.

Hindman, E. E., and B. P. Upadhyay (2002), Air pollution transport in the Himalayas of Nepal and Tibet during the 1995–1996 dry season, *Atmos. Environ.*, *36*(4), 727–739, doi:10.1016/S1352-2310(01)00495-2.

Hitzenberger, R. (2006), Intercomparison of thermal and optical measurement methods for elemental carbon and black carbon at an urban location, *Environ. Sci. Technol.*, *40*, 6377–6383, doi:10.1021/es051228v.

Hsu, N. C., J. R. Herman, and S.-C. Tsay (2003), Radiative impacts from biomass burning in the presence of clouds during boreal spring in southeast Asia, *Geophys. Res. Lett.*, *30*(5), 1224, doi:10.1029/2002GL016485.

Hyvärinen, A.-P., H. Lihavainen, M. Komppula, V. P. Sharma, V.-M. Kerminen, T. S. Panwar, and Y. Viisanen (2009), Continuous measurements of optical properties of atmospheric aerosols in Mukteshwar, northern India, *J. Geophys. Res.*, *114*, D08207, doi:10.1029/2008JD011489.

Intergovernmental Panel on Climate Change (IPCC) (2007), *Climate Change 2007: The Physical Science Basis. Contribution of Working Group I to the Fourth Assessment Report of the Intergovernmental Panel on Climate Change*, edited by S. Solomon et al., Cambridge Univ. Press, Cambridge, U. K.

Jacobson, M. Z. (2001), Strong radiative heating due to the mixing state of black carbon in atmospheric aerosols, *Nature*, *409*, 695–697, doi:10.1038/35055518.

Jacobson, M. Z. (2004), Climate response of fossil fuel and biofuel soot, accounting for soots feedback to snow and sea ice albedo and emissivity, *J. Geophys. Res.*, *109*, D21201, doi:10.1029/2004JD004945.

Kalthoff, N., H. J. Binder, M. Kossmann, R. Vogtlin, U. Corsmeier, F. Fielder, and H. Schlager (1998), Temporal evolution and spatial variation of the boundary layer over complex terrain, *Atmos. Environ.*, *32*, 1179–1194, doi:1352-2310/98.

Kanakidou, M., et al. (2005), Organic aerosol and global climate modelling: A review, *Atmos. Chem. Phys.*, *5*, 1053–1123, doi:10.5194/acp-5-1053-2005.

Koch, D., and J. Hansen (2005), Distant origins of Arctic black carbon: A Goddard Institute for Space Studies ModelE experiment, *J. Geophys. Res.*, *110*, D04204, doi:10.1029/2004JD005296.

Kossmann, M., R. Vogtlin, U. Corsmeier, B. Vogel, H. J. Binder, N. Kalthoff, and F. Beyrich (1998), Aspects of the convective boundary layer structure over complex terrain, *Atmos. Environ.*, *32*, 1323–1348, doi:1352-2310/98.

Kossmann, M., U. Corsmeier, S. F. J. deWekker, F. Fielder, R. Vogtlin, N. Kalthoff, H. Gusten, and B. Neininger (1999), Observations of handover processes between the atmospheric boundary layer and the free troposphere over mountainous terrain, *Contrib. Atmos. Phys.*, *72*, 329–350, doi:0005-8173/99/040329-22.

Krishna Moorthy, K., S. Suresh Babu, and S. K. Satheesh (2007), Temporal heterogeneity in aerosol characteristics and the resulting radiative impact at a tropical coastal station: Part 1: Microphysical and optical properties, *Ann. Geophys.*, *25*(11), 2293–2308, doi:10.5194/angeo-25-2293-2007.

Kulkarni, A. V., I. M. Bahuguna, B. P. Rathore, S. K. Singh, S. S. Randhawa, R. K. Sood, and S. Dhar (2007), Glacial retreat in Himalaya using Indian Remote Sensing Satellite data, *Curr. Sci.*, *92*(1), 69–74.

Lau, K. M., M. K. Kim, and K. M. Kim (2006), Asian summer monsoon anomalies induced by aerosol direct forcing: The role of the Tibetan Plateau, *Clim. Dyn.*, *26*, 855–864, doi:10.1007/s00382-006-0114-z.

Lau, K.-M., et al. (2008), The Joint Aerosol Monsoon Experiment: A new challenge for monsoon climate research, *Bull. Am. Meteorol. Soc.*, *89*, 369–383, doi:10.1175/BAMS-89-3-369.

Lawrence, M. G., and J. Lelieveld (2010), Atmospheric pollutant outflow from southern Asia: A review, *Atmos. Chem. Phys.*, *10*, 11,017–11,096, doi:10.5194/acp-10-11017-2010.

Marenco, F., et al. (2006), Characterization of atmospheric aerosols at Monte Cimone, Italy, during summer 2004: Source apportionment and transport mechanisms, *J. Geophys. Res.*, *111*, D24202, doi:10.1029/2006JD007145.

Marinoni, A., et al. (2010), Aerosol mass and black carbon concentrations, a two year record at NCO-P (5079 m, Southern Himalayas), *Atmos. Chem. Phys.*, *10*, 8551–8562, doi:10.5194/acp-10-8551-2010.

Meehl, G. A., J. M. Arblaster, and W. D. Collins (2008), Effects of black carbon aerosols on the Indian monsoon, *J. Clim.*, *21*, 2869–2882, doi:10.1175/2007JCLI1777.1.

Menon, S., J. Hansen, L. Nazarenko, and Y. Luo (2002), Climate effects of black carbon aerosols in China and India, *Science*, *297*, 2250–2253, doi:10.1126/science.1075159.

Mikhailov, E. F., S. S. Vlasenko, I. A. Podgorny, V. Ramanathan, and C. E. Corrigan (2006), Optical properties of soot-water drop agglomerates: An experimental study, *J. Geophys. Res.*, *111*, D07209, doi:10.1029/2005JD006389.

Ming, J., H. Cachier, C. Xiao, D. Qin, S. Kang, S. Hou, and J. Xu (2008), Black carbon record based on a shallow Himalayan ice core and its climatic implications, *Atmos. Chem. Phys.*, *8*, 1343–1352, doi:10.5194/acp-8-1343-2008.

Ming, J., C. Xiao, J. Sun, S. Kang, and P. Bonasoni (2010), Carbonaceous particles in the atmosphere and precipitation of the Nam Co region, central Tibet, *J. Environ. Sci.*, *22*(11), 1748–1756, doi:10.1016/S1001-0742(09)60315-6.

Moorthy, K. K., and S. S. Babu (2006), Aerosol black carbon over Bay of Bengal observed from an island location, Port Blair: Temporal features and long-range transport, *J. Geophys. Res.*, *111*, D17205, doi:10.1029/2005JD006855.

Moorthy, K. K., S. S. Babu, S. V. Sunilkumar, P. K. Gupta, and B. S. Gera (2004), Altitude profiles of aerosol BC, derived from aircraft measurements over an inland urban location in India, *Geophys. Res. Lett.*, *31*, L22103, doi:10.1029/2004GL021336.

Moorthy, K. K., S. K. Satheesh, S. S. Babu, and C. B. S. Dutt (2008), Integrated Campaign for Aerosols, gases and Radiation Budget (ICARB): An overview, *J. Earth Syst. Sci.*, *117*, 243–262, doi:10.1007/s12040-008-0029-7.

Moorthy, K. K., V. S. Nair, S. S. Babu, and S. K. Satheesh (2009), Spatial and vertical heterogeneities of aerosol radiative forcing over the oceanic regions surrounding the Indian peninsula: Climate implications, *Q. J. R. Meteorol. Soc.*, *135*, 2131–2145, doi:10.1002/qj.525.

Moy, L. A., R. R. Dickerson, and W. F. Ryan (1994), Relationship between back trajectories and tropospheric trace gas concentrations in rural Virginia, *Atmos. Environ.*, *28*, 2789–2800, doi:10.1016/1352-2310(94)90082-5.

Nair, V. S., et al. (2007), Wintertime aerosol characteristics over the Indo-Gangetic Plain (IGP): Impacts of local boundary layer processes and long-range transport, *J. Geophys. Res.*, *112*, D13205, doi:10.1029/2006JD008099.

Nair, V. S., K. K. Moorthy, S. S. Babu, and S. K. Satheesh (2009), Optical and physical properties of atmospheric aerosols over the Bay of Bengal during ICARB, *J. Atmos. Sci.*, *66*(9), 2640–2658, doi:10.1175/2009JAS3032.1.

Novakov, T., V. Ramanathan, J. Hansen, T. Kirchstetter, M. Sato, J. Sinton, and J. Sathaye (2003), Large historical changes of fossil-fuel black carbon emissions, *Geophys. Res. Lett.*, *30*(6), 1324, doi:10.1029/2002GL016345.

Nyeki, S., U. Baltensperger, I. Colbeck, D. T. Jost, E. Weingartner, and H. W. Gäggeler (1998), The Jungfraujoch high-alpine research station (3454 m) as a background clean continental site for the measurement

of aerosol parameters, *J. Geophys. Res.*, *103*, 6097–6107, doi:10.1029/97JD03123.

Pant, P., P. Hegde, U. C. Dumka, R. Sagar, S. K. Satheesh, K. K. Moorthy, A. Saha, and M. K. Srivastava (2006), Aerosol characteristics at a high-altitude location in central Himalayas: Optical properties and radiative forcing, *J. Geophys. Res.*, *111*, D17206, doi:10.1029/2005JD006768.

Pathak, B., G. Kalita, K. Bhuyan, P. K. Bhuyan, and K. K. Moorthy (2010), Aerosol temporal characteristics and its impact on shortwave radiative forcing at a location in the northeast of India, *J. Geophys. Res.*, *115*, D19204, doi:10.1029/2009JD013462.

Penner, J. E., C. C. Chuang, and K. Grant (1998), Climate forcing by carbonaceous and sulfate aerosols, *Clim. Dyn.*, *14*, 839–851, doi:10.1007/s003820050259.

Rai, K., A. K. Sarkar, and A. P. Mitra (2002), Chemical characterization of aerosols at NPL, Delhi, *IASTA Bull. Spec. lssue*, *14*(1), 155–158.

Ramanathan, V., and G. Carmichael (2008), Global and regional climate changes due to black carbon, *Nat. Geosci.*, *1*, 221–227, doi:10.1038/ngeo156.

Ramanathan, V., and P. J. Crutzen (2003), Atmospheric brown clouds, *Atmos. Environ.*, *37*, 4033–4035, doi:10.1016/S1352-2310(03)00536-3.

Ramanathan, V., et al. (2001), Indian Ocean experiment: An integrated analysis of the climate forcing and effects of the great Indo-Asian haze, *J. Geophys. Res.*, *106*, 28,371–28,398, doi:10.1029/2001JD900133.

Ramanathan, V., et al. (2007), Atmospheric brown clouds: Hemispherical and regional variations in long-range transport, absorption, and radiative forcing, *J. Geophys. Res.*, *112*, D22S21, doi:10.1029/2006JD008124.

Safai, P., S. Kewat, P. Praveen, P. Rao, G. Momin, K. Ali, and P. Devara (2007), Seasonal variation of black carbon aerosols over a tropical urban city of Pune, India, *Atmos. Environ.*, *41*(13), 2699–2709, doi:10.1016/j.atmosenv.2006.11.044.

Satheesh, S. K., K. K. Moorthy, S. S. Babu, V. Vinoj, and C. B. S. Dutt (2008), Climate implications of large warming by elevated aerosol over India, *Geophys. Res. Lett.*, *35*, L19809, doi:10.1029/2008GL034944.

Satheesh, S. K., V. Vinoj, and K. K. Moorthy (2011), Weekly periodicities of aerosol properties observed at an urban location in India, *Atmos. Res.*, *101*, 307–313, doi:10.1016/j.atmosres.2011.03.003.

Schmid, O., P. Artaxo, W. P. Arnott, D. Chand, L. V. Gatti, G. P. Frank, A. Hoffer, M. Schnaiter, and M. O. Andreae (2006), Spectral light absorption by ambient aerosols influenced by biomass burning in the Amazon Basin. I: Comparison and field calibration of absorption measurement techniques, *Atmos. Chem. Phys.*, *6*, 3443–3462, doi:10.5194/acp-6-3443-2006.

Seibert, P., H. Kromp-Kolb, U. Baltensperger, D. T. Jost, M. Schwikowski, A. Kasper, and H. Puxbaum (1994), Trajectory analysis of aerosol measurements at high alpine sites, in *Proceedings of the EUROTRAC Symposium*, edited by P. M. Borrell et al., pp. 689–693, SPB Acad., Hague, Netherlands.

Seinfeld, J. (2008), Black carbon and brown clouds, *Nat. Geosci.*, *1*, 15–16, doi:10.1038/ngeo.2007.62.

Sharma, S., D. Lavoué, H. Cachier, L. A. Barrie, and S. L. Gong (2004), Long-term trends of the black carbon concentrations in the Canadian Arctic, *J. Geophys. Res.*, *109*, D15203, doi:10.1029/2003JD004331.

Shaw, G. E. (2007), Aerosols at a mountaintop observatory in Arizona, *J. Geophys. Res.*, *112*, D07206, doi:10.1029/2005JD006893.

Sirois, A., and J. W. Bottenheim (1995), Use of backward trajectories to interpret the 5-year record of PAN and O_3 ambient air concentrations at Kejimkujil national Park, *J. Geophys. Res.*, *100*, 2867–2881, doi:10.1029/94JD02951.

Stohl, A., et al. (2006), Pan-Arctic enhancements of light absorbing aerosol concentrations due to North American boreal forest fires during summer 2004, *J. Geophys. Res.*, *111*, D22214, doi:10.1029/2006JD007216.

Stull, R. B. (1988), *An Introduction to Boundary Layer Meteorology*, Kluwer Acad., Dordrecht, Netherlands.

Sun, J., and P. A. Ariya (2006), Atmospheric organic and bio-aerosols as cloud condensation nuclei (CCN): A review, *Atmos. Environ.*, *40*, 795–820, doi:10.1016/j.atmosenv.2005.05.052.

Tomasi, C., et al. (2007), Aerosols in polar regions: A historical overview based on optical depth and in situ observations, *J. Geophys. Res.*, *112*, D16205, doi:10.1029/2007JD008432.

Vaughan, J. M., R. H. Maryon, and N. J. Geddes (2002), Comparison of atmospheric aerosol backscattering and air mass back trajectories, *Meteorol. Atmos. Phys.*, *79*, 33–46, doi:10.1007/s703-002-8227-6.

Venzac, H., K. Sellegri, P. Villani, D. Picard, and P. Laj (2009), Seasonal variation of aerosol size distribution at Puy de Dôme (1465 m a.s.l., central France), *Atmos. Chem. Phys.*, *9*, 1465–1478, doi:10.5194/acp-9-1465-2009.

Verma, N., S. P. Bagare, S. S. Ningombam, and R. B. Singh (2010), Aerosol optical properties retrieved using Skyradiometer at Hanle in western Himalayas, *J. Atmos. Sol. Terr. Phys.*, *72*, 115–124, doi:10.1016/j.jastp.2009.10.016.

Warren, S., and W. Wiscombe (1980), A model for the spectral albedo of snow. II: Snow containing atmospheric aerosols, *J. Atmos. Sci.*, *37*, 2734–2745, doi:10.1175/1520-0469(1980)037<2734:AMFTSA>2.0.CO;2.

Weingartner, E., H. Saathoff, M. Schnaiter, N. Streit, B. Bitnar, and U. Baltensperger (2003), Absorption of light by soot particles: Determination of the absorption coefficient by means of aethalometers, *J. Aerosol Sci.*, *34*, 1445–1463, doi:10.1016/S0021-8502(03)00359-8.

Welton, E. J., K. J. Voss, P. K. Quinn, P. J. Flatau, K. Markowicz, J. R. Campbell, J. D. Spinhirne, H. R. Gordon, and J. E. Johnson (2002), Measurements of aerosol vertical profiles and optical properties during INDOEX 1999 using micropulse lidars, *J. Geophys. Res.*, *107*(D19), 8019, doi:10.1029/2000JD000038.

S. P. Bagare, B. C. Bhatt, V. K. Gaur, T. P. Prabhu, and N. S. Singh, Indian Institute of Astro Physics, Bangalore 560 034, India.

S. S. Babu, J. P. Chaubey, M. M. Gogoi, S. K. Kompalli, K. K. Moorthy, and V. Sreekanth, Space Physics Laboratory, Vikram Sarabhai Space Centre, Trivandrum 695 022, India. (s_sureshbabu@vssc.gov.in)